AFRL-VA-WP-TP-2002-304

CONCEPTS FOR CONSTRAINED CONTROL ALLOCATION OF MIXED QUADRATIC AND LINEAR EFFECTORS

David B. Doman
Andrew G. Sparks

APRIL 2002

Approved for public release; distribution is unlimited.

AIR VEHICLES DIRECTORATE
AIR FORCE RESEARCH LABORATORY
AIR FORCE MATERIEL COMMAND
WRIGHT-PATTERSON AIR FORCE BASE, OH 45433-7542

REPORT DOCUMENTATION PAGE

Form Approved
OMB No. 0704-0188

1. REPORT DATE *(DD-MM-YY)*	2. REPORT TYPE	3. DATES COVERED *(From - To)*
April 2002	Conference Paper Preprint	08/01/2001 – 01/20/2002

4. TITLE AND SUBTITLE
CONCEPTS FOR CONSTRAINED CONTROL ALLOCATION OF MIXED QUADRATIC AND LINEAR EFFECTORS

5a. CONTRACT NUMBER
In-house

5b. GRANT NUMBER

5c. PROGRAM ELEMENT NUMBER
61102F

6. AUTHOR(S)
David B. Doman
Andrew G. Sparks

5d. PROJECT NUMBER
2304

5e. TASK NUMBER
N2

5f. WORK UNIT NUMBER
01

7. PERFORMING ORGANIZATION NAME(S) AND ADDRESS(ES)
Control Theory Optimization Branch (AFRL/VACA)
Control Sciences Division
Air Vehicles Directorate
Air Force Research Laboratory, Air Force Materiel Command
Wright-Patterson Air Force Base, OH 45433-7542

8. PERFORMING ORGANIZATION REPORT NUMBER
AFRL-VA-WP-TP-2002-304

9. SPONSORING/MONITORING AGENCY NAME(S) AND ADDRESS(ES)
Air Vehicles Directorate
Air Force Research Laboratory
Air Force Materiel Command
Wright-Patterson AFB, OH 45433-7542

10. SPONSORING/MONITORING AGENCY ACRONYM(S)
AFRL/VACA

11. SPONSORING/MONITORING AGENCY REPORT NUMBER(S)
AFRL-VA-WP-TP-2002-304

12. DISTRIBUTION/AVAILABILITY STATEMENT
Approved for public release; distribution is unlimited.

13. SUPPLEMENTARY NOTES
This material is declared a work of the U.S. Government and is not subject to copyright protection in the United States.

Paper to be presented at the America Control Conference, May 8 through 10, 2002. This document was submitted to DTIC with color content. When the document was processed by DTIC, the color content was lost.

14. ABSTRACT
Concepts for new constrained control allocation strategies are developed that deal with systems where moments are nonlinearly related to effector deflections such as those encountered in the case of yawing moment contributions from left-right effector pairs on aircraft. These concepts are illustrated by considering single and multiple left-right pair effector mixing problems for moments that lie in the roll-yaw moment plane. Methods for generating the boundary of an attainable moment set for a class of multiple nonlinear effectors and for clipping unattainable moment commands with axis prioritization are presented.

15. SUBJECT TERMS

16. SECURITY CLASSIFICATION OF: a. REPORT	b. ABSTRACT	c. THIS PAGE	17. LIMITATION OF ABSTRACT:	18. NUMBER OF PAGES	19a. NAME OF RESPONSIBLE PERSON (Monitor)
Unclassified	Unclassified	Unclassified	SAR	12	Dr. David B. Doman **19b. TELEPHONE NUMBER** *(Include Area Code)* (937) 255-8451

HES&S 31-15093-1

Standard Form 298 (Rev. 8-98)
Prescribed by ANSI Std. Z39-18

Concepts for Constrained Control Allocation of Mixed Quadratic and Linear Effectors

David B. Doman and Andrew G. Sparks
AFRL/VACA
Control Theory and Optimization Branch
Wright-Patterson AFB, OH 45433-7531
Email: david.doman@wpafb.af.mil/andrew.sparks@wpafb.af.mil

Abstract

Concepts for new constrained control allocation strategies are developed that deal with systems where moments are nonlinearly related to effector deflections such as those encountered in the case of yawing moment contributions from left-right effector pairs on aircraft. These concepts are illustrated by considering single and multiple left-right pair effector mixing problems for moments that lie in the roll-yaw moment plane. Methods for generating the boundary of an attainable moment set for a class of multiple non-linear effectors and for clipping unattainable moment commands with axis prioritization are presented.

1 Introduction

Left-right aerodynamic surfaces such as ailerons, flaps and elevons on aerospace vehicles often have non-linear contributions to the total vehicle yawing moment. Since these surfaces are not normally used as primary yaw axis effectors, these non-linear contributions are often ignored and their effects are treated as disturbances that are rejected by a feedback control system. In cases where the effectiveness of the primary yaw axis effector is degraded due to failures or as a result of being in the wake of the body at high angles of attack, these secondary nonlinear effects become important.

Numerous control allocation and control effector mixing algorithms have been developed over the past decade and excellent survey papers have been written that point out the strengths and weaknesses of the existing approaches[1, 2]. These control mixing and control allocation algorithms are capable of dealing with systems where the moments were linearly related to control effector positions and had the ability to account for constraints on those positions. Some of these algorithms generate constrained control effector commands that ensure that the effectors are never driven beyond their physical limits. Most of the algorithms, however, assume that linear relationships exist between the pseudo-commands (i.e. controlled variable commands) and the effector positions. While this assumption is at least locally valid for many of the control surfaces on found on aircraft, there are exceptions.

One particular case where this assumption can result in incorrect control surface deflections and return unnecessarily conservative results involves the use of left-right aerodynamic control surfaces on aircraft. Examples of left-right aerodynamic surfaces include left-right elevators and left-right ailerons. This type of surface can generally produce pitching, rolling and yawing moments. While these surfaces normally produce pitching and rolling moments that are locally linear in control surface deflection, they can have a highly nonlinear contribution to the yawing moment especially when parasitic drag dominates induced drag effects.

In particular, these surfaces can generate yawing moments that are of the same sign whether they are deflected up or down. This is because they generate a drag force on the side of the vehicle on which they are located regardless of whether they deflected in the positive or negative direction. The yawing moments generated by these effectors are usually small when compared to a primary yaw-axis effector like a rudder; however, their effects can become significant when a rudder fails or when the aircraft is operating at high angles of attack where flow over the rudder is interrupted by the body.

This particular nonlinearity is used as motivation and serves as an example for the concepts explored in this paper. Methods for generating the boundary of an attainable moment set for a class of multiple non-linear effectors and for clipping unattainable moment commands with axis prioritization are presented. The techniques presented are applicable to more general nonlinear control allocation problems.

2 Attainable Moment Set for a Single Left-Right Effector Pair

Durham[3] developed and subsequently refined methods for determining attainable moment sets (AMS) for effectors that generate moments $\mathbf{M}$ that are linear functions $\mathbf{M} = \mathbf{B}\boldsymbol{\delta}$ of the effector positions $\boldsymbol{\delta}$ subject to constraints on those positions $\boldsymbol{\delta} = \{\delta | \underline{\delta} \leq \delta \leq \bar{\delta}\}$. The general solution to finding the attainable moment set for an over-actuated linear system with position constraints involves constructing a polyhedron in moment space. Potential vertices are are constructed by locking all control effectors at their extreme positions in all possible combinations while allowing two effectors to traverse the range of their possible positions. Durham's algorithm connected the vertices to form potential boundary facets and determined which facets were on the boundary of the AMS.

Left-right (LR) pairs of effectors such as ailerons, elevators and flaps as mentioned previously, generate non-linear contributions to the vehicle yawing moment. Figure 1 shows the yawing moment that is generated by deflecting the right elevon of a particular lifting body vehicle. One can see that a parabolic fit provides an adequate approximation of the original data. Generation of linear fits to this data for use in a conventional control allocator that assume a linear relationship between the moments and control effector deflections is problematic. This is because lines fitted using either negative deflection or positive deflection data results in lines with slopes of opposite signs. Furthermore, since no single line can accurately model the data and no matter which line is selected, the sign of the yawing moment estimate will be incorrect half of the time.

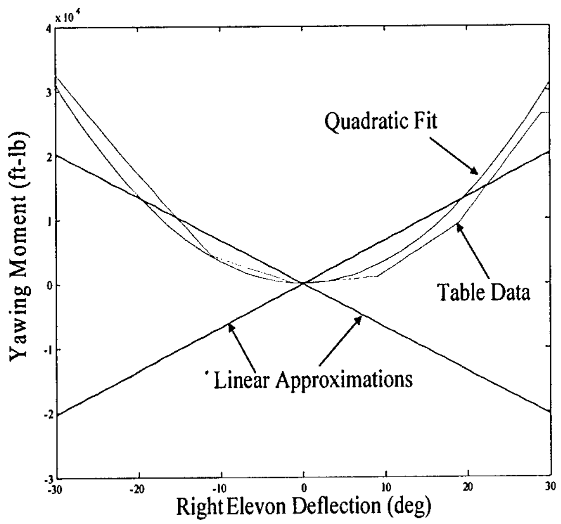

Figure 1: Yawing Moment due to Right Elevon Deflection

Here we examine a case where a LR pair of elevons exerts yawing moment N that is proportional to the square of deflection and rolling moment L that is a linear function of deflection

$$\begin{aligned} N &= N_{le^2}\delta_{le}^2 + N_{re^2}\delta_{re}^2, \\ L &= L_{le}\delta_{le} + L_{re}\delta_{re}. \end{aligned} \tag{1}$$

From the curve fits to aerodynamic data for a lifting body model at a subsonic flight condition, we select $N_{re^2} = -N_{le^2} = 34 ft - lb/deg^2$ and $L_{re} = -L_{le} = -4610 ft - lb/deg$. The AMS is generated by holding each surface at a fixed deflection while allowing the other surface to vary over its range of possible values and is shown in Figure 2.

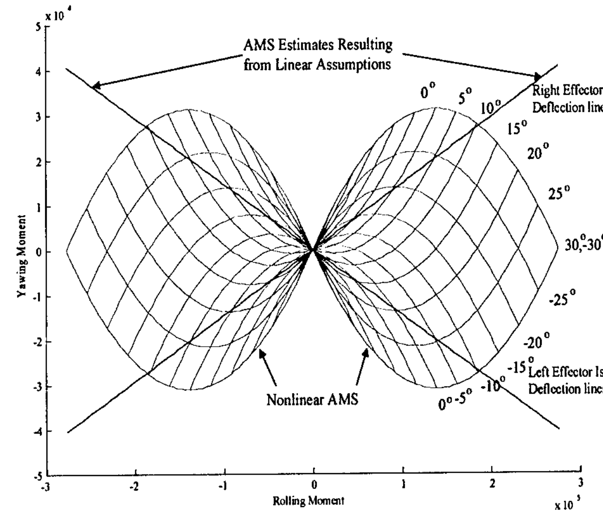

Figure 2: Nonlinear AMS and Lines of Constant Deflection in the Roll-Yaw Moment Plane

The AMS is also shown for the yawing moment as a linear function of the deflections. For the linear approximation we fit data over half of the range of deflections to obtain $N_{le} = -N_{re} = \pm 676 ft - lb/deg$. The sign ambiguity results from the yawing moment derivatives' dependency on the sign of the deflections; either choice of sign will only yield a yawing moment with the correct sign over half of the deflection range. The AMS for the linear case shows that a control allocator that incorrectly assumes a linear relationship between the yawing moment and the effector deflections will be constrained to rolling and yawing moments that lie on one of two lines in the roll-yaw plane. The AMS for the improved effector model shows that larger regions in the roll-yaw plane are reachable and the intersection of lines of constant effector deflection define the proper blend of effectors required to achieve a particular rolling and yawing moment that lies within the AMS.

3 Clipping Infeasible Moment Commands

It is interesting to note that it is not possible to generate yawing moments without generating a corresponding rolling moment with one set of left-right effectors. This point begs the question of how to clip rolling and yawing moment commands that lie outside of the AMS. When a moment command requires violation of an effector position constraint, Durham[4] suggested that the direction of a moment command should be preserved and that the command should be clipped such that the commanded moment vector touched the edge of the AMS.

For the case under consideration, one can see that preserving the direction of a pure yawing moment command will result in the command being clipped to zero. A proposed method for clipping commands that lie outside of the AMS that provides the ability to prioritize moments is given below. When a command is infeasible, we find a way of choosing a point on the boundary of the AMS that is closest in some sense to the infeasible command.

We propose to minimize the sum of weighted square distances between the AMS boundary and the desired point in moment space

$$\min_{L} \left[(L_d - L)^2 + w(N_d - N_b(L))^2\right], \qquad (2)$$

where w is a weighting factor that can be used to weight the relative importance of achieving the rolling or yawing moment and $N_b(L)$ is the equation for the AMS boundary which is closest to the desired yawing moment N_d. The first order necessary condition for an extremum of the cost function is

$$L - L_d + wN_b'(L)(N_b(L) - N_d) = 0, \qquad (3)$$

which can be solved for L either numerically or analytically in special cases. Figure 3 shows the effect of varying weights in the cost function for a hypothetical infeasible moment command. Note that when $w = 0$ the desired rolling moment is achieved; as w is increased, the error in yawing moment is reduced to as small of a value as possible while the rolling moment error increases. This type of strategy may be useful if other effectors are available to reduce the undesired rolling moment if a particular left-right pair must be used as a primary yaw-axis effector.

To account for nonlinear effectors one must consider the most general form of the control allocation problem. This problem reduces to a constrained root-finding problem that can be solved using clipping logic as a pre-processing step coupled with standard root-finding techniques. Alternatively nonlinear programming techniques can be used, although it is likely that

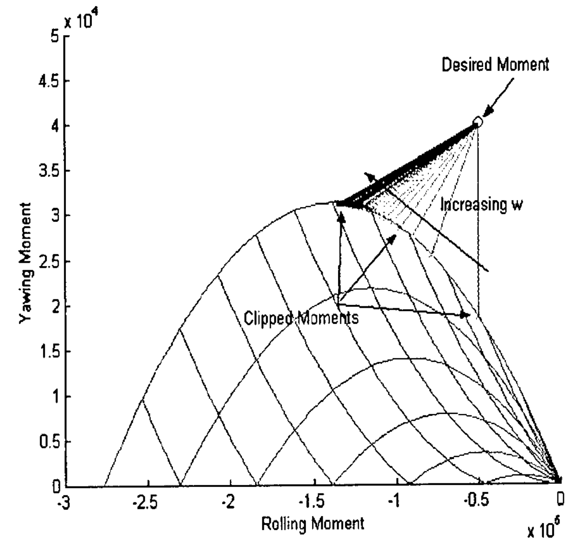

Figure 3: Clipping of Infeasible Moment Command

nonlinear programming may be too slow for on-line control allocation. In order to use root-finding techniques, one must first determine if a moment command is feasible or lies within the AMS boundary. If the command is feasible standard root-finding techniques can be used. If a command is not feasible, it must be clipped at the AMS boundary and the axis prioritization method presented in the previous section provides a means for performing this operation.

4 AMS Boundaries for Multiple Effectors

The generation of an AMS for a single LR pair is relatively straightforward. Here we would like to develop a method for generating the AMS for multiple LR effector pairs. To illustrate how this might be accomplished we consider the rolling and yawing moments that can be generated by two LR effector pairs of the form

$$\begin{aligned} N_T &= N_1\delta_1^2 + N_2\delta_2^2 + N_3\delta_3^2 + N_4\delta_4^2, \\ L_T &= L_1\delta_1 + L_2\delta_2 + L_3\delta_3 + L_4\delta_4, \end{aligned} \qquad (4)$$

and for the purposes of example we let $N_1 = -N_2 = 34 ft - lb/deg^2$, $N_3 = -N_4 = N_1/25$, $L_1 = -L_2 = -4610 ft - lb/deg$, and $L_3 = -L_4 = L_1/5$. We set all effector deflection limits to $\pm 30 deg$. To generate the upper AMS boundaries for the 1-2 effector pair we set $\delta_3 = \delta_4 = 0$, $\delta_1 = 30$ $\delta_1 = -30$, and let δ_2 vary continously between ± 30. The lower boundaries and the boundaries for the 3-4 effector pair can be generated in a similar fashion. To generate the AMS boundary for both of the LR pairs acting together, one may add the AMS of the 3-4 pair to each point on the 1-2

AMS boundary. Figure 4 shows the effect of performing this operation. In principle, the AMS boundary could be generated by exhaustion by moving the origin of the 3-4 AMS boundary to each point on the 1-2 AMS boundary and drawing a composite AMS for the 1-2-3-4 effectors by drawing a curve that touches the extremal points in the roll-yaw plane. Such a procedure would clearly be inefficient.

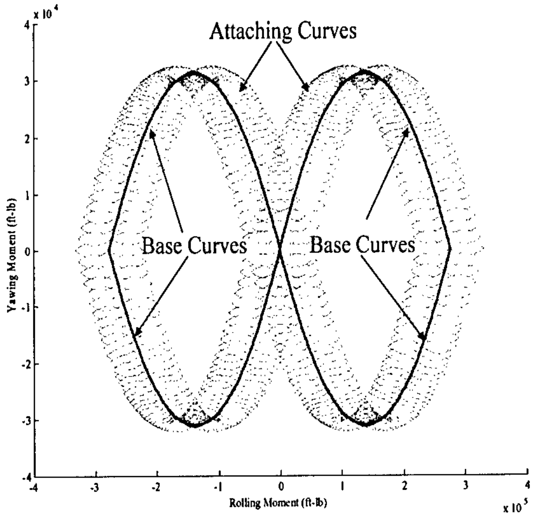

Figure 4: Generation of AMS by Superposition

It is therefore natural to ask if there exists a method or condition that relates the AMS of each LR pair considered individually to points on the composite boundary approximated by the outline of Figure 4. The condition for a point on the boundary turns out to be related to the slope of the AMS boundary curves. For convenience we shall consider the top left quadrants of the two boundaries and denote the boundary curve for the first LR pair $f(x)$ and the boundary curve for the second LR pair $g(x)$ as shown in Figure 4. In order to generate the composite boundary, one can generate a number of auxiliary functions $h(x,\overline{x}) = g(x-\overline{x}) + f(\overline{x})$ where the point $(\overline{x}, f(\overline{x}))$ is a point at which the boundary curve for the second LR pair attaches to the boundary curve for the first LR pair.

Definition 1 *An attachment point to $f(x)$ is a point $P(\overline{x}, f(\overline{x}))$ to which the origin of a curve $g(x)$ is translated for the purpose of calculating values of a new function that is composed of the two original functions $h(x,\overline{x}) = g(x-\overline{x}) + f(\overline{x})$*

Hence, $h(x,\overline{x})$ shifts the origin of the original curve $g(x)$ to a point on $f(x)$ at $x = \overline{x}$. We define points on

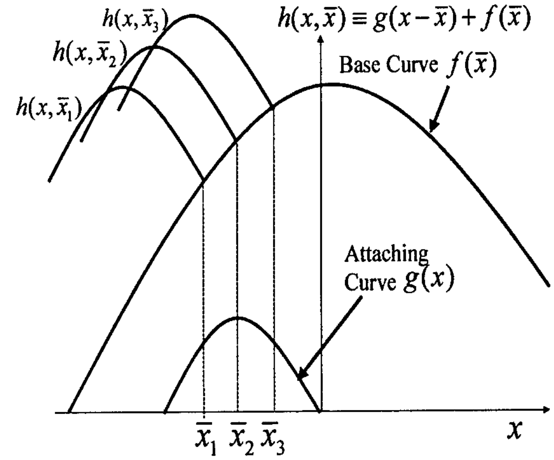

Figure 5: Generation of the AMS Boundary

the composite boundary as those that produce maximum or minimum values of the $h(x,\overline{x})$ as $\overline{x}$ is varied over its range of physically realizable values.

Definition 2 *The composite boundary $b(x)$ generated from all physically realizable values of $h(x,\overline{x}) = g(x-\overline{x}) + f(\overline{x})$ is defined as the set of extremal values of $h(x,\overline{x})$ for $\{\overline{x} \in \mathbb{R} | x_{min_f} \leq \overline{x} \leq x_{max_f}\}$ and $\{x \in \mathbb{R} | x_{min_f} + x_{min_g} \leq (x-\overline{x}) \leq x_{max_f} + x_{max_g}\}$ where x_{min_f}, x_{min_g} and x_{max_f}, x_{max_g} are the minimum and maximum values of x and $\overline{x}$ for which $f(\overline{x})$ and $g(x)$ physically exist.*

Theorem 1 states a necessary condition for a point to lie on the composite boundary.

Theorem 1 *If $f(x)$ and $g(x)$ are C^1 with monotonic slopes and $h(x,\overline{x}) = g(x-\overline{x}) + f(\overline{x})$ then for any $x \in \{x \in \mathbb{R} | x_{min_f} + x_{min_g} \leq (x-\overline{x}^*) \leq x_{max_f} + x_{max_g}\}$ a point on the composite boundary,$P(x, h(x,\overline{x}^*))$ satisfies the following condition*

$$\frac{\partial}{\partial(x-\overline{x})} g(x-\overline{x})\bigg|_{\overline{x}=\overline{x}^*} = \frac{\partial}{\partial \overline{x}} f(\overline{x})\bigg|_{\overline{x}=\overline{x}*} . \qquad (5)$$

Proof: By definition points on the composite boundary are extremal values of $h(x,\overline{x}) = g(x-\overline{x}) + f(\overline{x})$. It is assumed that $f(x)$ and $g(x)$ have continuous derivatives and that these derivatives are monotonic functions of x. At any given value of x, we are interested in finding an attachment point $P(\overline{x}^*, f(\overline{x}^*)$ that will result in an extremal value for the composite function $h(x,\overline{x})$. The first order necessary condition for an extremum of $h(x,\overline{x})$ is

$$\frac{\partial}{\partial \overline{x}} h(x,\overline{x})\bigg|_{\overline{x}=\overline{x}^*} = 0. \qquad (6)$$

Applying the chain rule for derivatives and after routine manipulations, it is easy to verify that Equation 6 is equivalent to Equation 5. Since the slopes of $f(x)$ and $g(x)$ are monotonic, there is one and only one value of $\overline{x}$ that satisfies Equation 5 and this value of $\overline{x}$ is defined as $\overline{x}^*$. ■

Remark 1 *If* $(x - \overline{x}^*) \geq x_{max_g}$ *then the boundary point is given by* $P[\overline{x}^* + x_{max_g}, h(x_{max_g}, \overline{x}^*)]$.

Remark 2 *If* $(x - \overline{x}^*) \leq x_{min_g}$ *then the boundary point is given by* $P[\overline{x}^* + x_{min_g}, h(x_{min_g}, \overline{x}^*)]$.

Theorem 1 and Remarks 1 and 2 collectively state that the point on $h(x, \overline{x})$ that has the same slope as $f(x)$ at the attachment point is a point on the composite boundary, as long as that point does not require violation of the effector position limits. Theorem 1 may be used as part of a process to determine the composite boundary by solving the Equation 5 for $\overline{x}^*$ as a function of x only. Contributions to the AMS from additional LR pairs can be accommodated by repeatedly applying this procedure. A similar procedure should provide a means for computing AMS volumes in moment space; however, the planar case was explored here for concept development.

5 Composite AMS Calculation

This section provides an example of how to calculate a section of a composite AMS boundary using Theorem 1. It is relatively easy to to generate segments of the AMS boundary for a single pair of left-right effectors. Theorem 1 provides a means for computing composite boundary segments given the AMS boundaries for single L-R pairs. We will now consider the case where the rolling and yawing moments produced by two sets of LR pairs as in Equation 4. Note that even though the contributions of the individual effectors to the yawing moment are non-linear, there is no coupling between the effectors. This implies that the total rolling and yawing moments that are achievable by using the 1-2 and 3-4 effector pairs together can be obtained by summing the contributions of the respective LR pairs

$$\begin{aligned} N_T &= N_{12} + N_{34}, \\ L_T &= L_{12} + L_{34}. \end{aligned} \tag{7}$$

In this example we consider the following parametric equations for the segment of the AMS boundary for the 1-2 effector pair alone in the second quadrant of the roll-yaw plane

$$\begin{aligned} N_{12} &= K_n\delta_1^2 - K_n\delta_{2_{max}}^2, \\ L_{12} &= K_l\delta_1 - K_l\delta_{2_{max}}, \end{aligned} \tag{8}$$

where $K_n = -34ft - lb/deg^2$, $K_l = 4610ft - lb/deg$ and $\delta_{2_{max}} = 30^o$. Note that all effector position limits are $\pm 30^o$ in this example. Equation 8 will generate a curve of constant effector deflection for $\delta_{2_{max}} = 30^o$ when N_{12} is plotted as a function of L_{12}. This curve is a segment of the AMS boundary for the 1-2 effector pair. Eliminating the parameter δ_1, and solving for $N_{12}(L_{12})$ one obtains

$$N_{12}(L_{12}) = \frac{K_n}{K_l^2}L_{12}^2 + \frac{2K_n\delta_{2_{max}}}{K_L}L_{12}. \tag{9}$$

Similarly one can generate an equation for the AMS boundary for the 3-4 effector pair acting alone. Again considering the AMS boundary in the second quadrant

$$N_{34}(L34) = \frac{C_n}{C_l^2}L_{34}^2 + \frac{2C_n\delta_{2_{max}}}{C_L}L_{34}, \tag{10}$$

where $C_n = K_n/4$ and $C_l = K_l/2$. Equations 9 and 10 can be plotted in the roll-yaw plane and for convenience; we eliminate the subscripts on L and treat it as the independent variable. Physical limits on L must be observed for the 1-2 and 3-4 pairs in order to test the conditions stated in Remarks 1 and 2. These limits are given by

$$\begin{aligned} L_{12_{max}} &= 0, \\ L_{12_{min}} = 2K_l\delta 1_{min} &= -276600ft - lb, \\ L_{34_{max}} &= 0, \\ L_{34_{min}} = 2C_l\delta 1_{min} &= -138300ft - lb. \end{aligned} \tag{11}$$

We now apply Theorem 1 and Remarks 1 and 2. First we arbitrarily choose the 1-2 curve as the base curve, which we will refer to as $N_{12}(\overline{L})$. The 3-4 boundary curve $N_{34}(L)$ is chosen as the attaching curve and the origin will in principle be shifted to all points on $N_{12}(\overline{L})$ viz. $N_{34}(L - \overline{L})$. Theorem 1 states that points on the composite boundary occur where the slopes of the base and attached curves are equal. The slopes of Equations 9 and 10 are given by

$$\frac{\partial N_{12}(\overline{L})}{\partial \overline{L}} = 2\frac{K_n}{K_l^2}(\overline{L} + K_l\delta_{2_{max}}), \tag{12}$$

$$\frac{\partial N_{34}(L - \overline{L})}{\partial (L - \overline{L})} = 2\frac{C_n}{C_l^2}((L - \overline{L}) + C_l\delta_{2_{max}}). \tag{13}$$

Setting Equations 12 and 13 equal and solving for the value of $\overline{L}$ that satisfies the equality, namely $\overline{L}^*$, one obtains

$$\overline{L}^* = \frac{\frac{C_n}{C_l^2}(L + C_l\delta_{2_{max}}) - \frac{K_n}{K_l}\delta_{2_{max}}}{\frac{K_n}{K_l^2} + \frac{C_n}{C_l^2}}. \tag{14}$$

Now that $\overline{L}^*$ can be written as a function of L only, one can write the equation for the composite boundary (without regard to position-limit imposed constraints on $L - \overline{L}^*$) as

$$
\begin{aligned}
N_B(L,\overline{L}^*) = {} & \frac{K_n}{K_l^2}\overline{L}^{*2} + 2\frac{K_n}{K_l}\delta_{2_{max}}\overline{L}^* \\
& + \frac{C_n}{C_l^2}(L-\overline{L}^*)^2 + 2\frac{C_n}{C_l}\delta_{2_{max}}(L-\overline{L}^*).
\end{aligned} \tag{15}
$$

Remarks 1 and 2 must now be applied to ensure that it is physically possible to move the control surfaces to points where the slopes are equal. If this is not physically possible, due to position limits on the effectors, the boundary point will be evaluated at the upper or lower limit of L for the effector-pair in question. In this case the attaching curve if the 3-4 AMS boundary whose upper and lower bounds on L are given in Equation 11. Applying Remark 1 we find that when $L - \overline{L}^* \geq L_{34_{max}}$, the boundary becomes a function of $\overline{L}^*$ only

$$
\begin{aligned}
N_B(\overline{L}^*) = {} & \frac{K_n}{K_l^2}\overline{L}^{*2} + 2\frac{K_n}{K_l}\delta_{2_{max}}\overline{L}^* \\
& + \frac{C_n}{C_l^2}(L_{34_{max}})^2 + 2\frac{C_n}{C_l}\delta_{2_{max}}(L_{34_{max}}).
\end{aligned} \tag{16}
$$

Similarly from Remark 2 we find that when $L - \overline{L}^* \leq L_{34_{min}}$

$$
\begin{aligned}
N_B(\overline{L}^*) = {} & \frac{K_n}{K_l^2}\overline{L}^{*2} + 2\frac{K_n}{K_l}\delta_{2_{max}}\overline{L}^* \\
& + \frac{C_n}{C_l^2}(L_{34_{min}})^2 + 2\frac{C_n}{C_l}\delta_{2_{max}}(L_{34_{min}}).
\end{aligned} \tag{17}
$$

Figure 5 shows the composite boundary segment $N_B(L, \overline{L}^*)$ for the example above. Construction of the other boundary segments will follow a similar procedure and opportunities to exploit symmetry obviously exist but were not considered here for brevity. Also, it is clear that as additional boundary segments are computed, there may be overlap in some regions and a method must be devised to choose the most liberal boundary segment at a given point.

6 Conclusion

Concepts for new constrained control allocation strategies were explored in this paper that deal with systems where moments are nonlinearly related to effector deflections, such as those encountered in the case of yawing moment contributions from left-right effector pairs on aircraft. The concepts were illustrated by considering single and multiple left-right pair effector mixing problems for moments that lie in the roll-yaw moment plane. The attainable moment sets for individual left-right effector pairs are relatively easy to construct, and

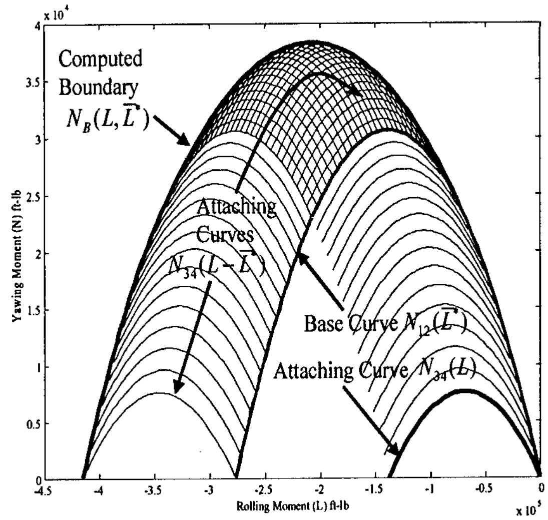

Figure 6: Composite Boundary Segment

a method was presented that allows one to construct a more complex composite boundary from the individual left-right pair attainable moment sets. Necessary conditions for points on the boundary of the attainable moment set for multiple left-right effector pairs were derived for the planar case where only two moments are specified. Extension of the theory to include necessary conditions for points on the boundary of the attainable moment set in 3-dimensional moment space presently remains an open but important problem. A method for clipping unattainable moment commands with axis prioritization was presented.

References

[1] A. B. Page and M. L. Steinberg, "A Closed-loop Comparison of Control Allocation Methods," in *Proceedings of the 2000 Guidance, Navigation and Control Conference*, AIAA 2000-4538, August 2000.

[2] M. Bodson, "Evaluation of Optimization Methods for Control Allocation," in *Proceedings of the 2001 Guidance, Navigation and Control Conference*, AIAA, August 2001.

[3] W. Durham, "Attainable moments for the constrained control allocation problem," *Journal of Guidance, Control and Dynamics*, vol. 17, no. 6, pp. 1371–1373, 1994.

[4] W. Durham, "Constrained control allocation: Three moment problem," *Journal of Guidance, Control and Dynamics*, vol. 16, no. 4, pp. 717–725, 1993.